Mixing in a Meandering Jet: A Markovian Approximation

Massimo Cencini

Dipartimento di Fisica, Università ''la Sapienza,'' and Istituto Nazionale Fisica della Materia, Unità di Roma, Rome, Italy

Guglielmo Lacorata

Dipartimento di Fisica, Università dell' Aquila, Coppito, and Istituto di Fisica dell'Atmosfera—CNR, Rome, Italy

Angelo Vulpiani

Dipartimento di Fisica, Università ''la Sapienza,'' and Istituto Nazionale Fisica della Materia, Unità di Roma, Rome, Italy

Enrico Zambianchi

Istituto di Meteorologia e Oceanografia, Istituto Universitario Navale, Naples, Italy

ABSTRACT

Mixing and transport in correspondence of a meandering jet are investigated. The large-scale flow field is a kinematically assigned streamfunction. Two basic mixing mechanisms are considered separately and in combination: deterministic chaotic advection induced by a time dependence of the flow, and turbulent diffusion described by means of a stochastic model for particle motion.

Rather than looking at the details of particle trajectories, fluid exchange is studied in terms of Markovian approximations. The 2D physical space accessible to fluid particles is subdivided into regions characterized by different Lagrangian behavior. From the observed transitions between regions it is possible to derive a number of relevant quantities characterizing transport and mixing in the studied flow regime, such as residence times, meridional mixing, and correlation functions. These estimated quantities are compared to the corresponding ones resulting from the actual simulations. The outcome of the comparison suggests the possibility of describing in a satisfactory way at least some of the mixing properties of the system through the very simplified approach of a first-order Markovian approximation, whereas other properties exhibit memory patterns of higher order.

1. Introduction

Western boundary current extensions typically exhibit a meandering jetlike flow pattern. The most renowned example of this is given by the meanders of the Gulf Stream extension, which have been investigated in their variability by means of both in situ and remotely sensed data [see, e.g., Watts (1983) for a survey of earlier studies, as well as Halliwell and Mooers (1983), Vazquez and Watts (1985), Cornillon et al. (1986), Tracey and Watts (1986), Kontoyiannis and Watts (1994), Lee (1994)].

These strong currents often separate regions of the oceans characterized by water masses, which are quite different in terms of their physical and biogeochemical characteristics. Consequently, they are associated with very sharp and localized property gradients; this makes the study of mixing processes across them particularly relevant also for interdisciplinary investigations. This is the case of the Gulf Stream (Bower et al. 1985; Bower and Lozier 1994), the Kuroshio, and the Brazil–Malvinas Current (Backus 1986).

A major mechanism for cross-frontal exchange in western boundary current extensions is represented by warm or cold core ring shedding at either side of the jet and then migrating into the opposite region across the jet itself. This has been clearly seen from satellite infrared imagery, and individual rings have been tracked by Lagrangian instruments [for a general review, see Olson (1991)]. However, RAFOS float data collected in the Gulf Stream (Bower and Rossby 1989) have drawn attention toward fluid exchange in the absence of rings,

Corresponding author address: Dr. Enrico Zambianchi, Istituto di Meteorologia e Oceanografia, Istituto Universitario Navale, Via Acton 38, 80133 Napoli, Italy.
E-mail: enrico@naval.uninav.it
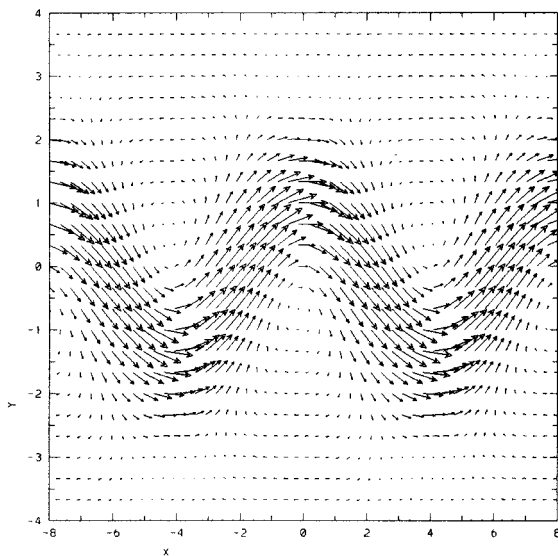
FIG. 1. Snapshot of the velocity field derived from the streamfunction (2) with $L = 7.5$, $B_0 = 1.2$, $c = 0.12$.

due to smaller-scale frontal mixing, which causes detrainment or entrainment from or into the surrounding waters [an excellent example is given by the RAFOS trajectories shown in Fig. 1 of Bower and Lozier (1994); see also the discussion therein].

The mixing properties of passive tracers across meandering jets have been investigated in the recent past by a number of authors, following essentially two different approaches. The first one is that of dynamical models, where the flow is produced by integrating the equations of motion, time dependence is typically produced by (barotropic or baroclinic) instability processes, and dissipation is present (e.g., Yang 1996). These models account for several mechanisms acting in mixing in the real ocean, even if sorting out single processes of interest may be sometimes complicated.

A second and simpler approach, the one followed in this paper, is that of kinematic models [Bower (1991, hereafter B91), Samelson (1992, hereafter S92), Dutkiewicz et al. (1993, hereafter DGO93), Duan and Wiggins (1996), for slightly different kinds of flows see also Lacorata et al. (1996)]. In such models the large-scale velocity field is represented by an assigned flow whose spatial and temporal characteristics mimic those observed in the ocean. However, the flow field may not be dynamically consistent in the sense of being a solution of the equations of motion, or of conserving, for example, potential vorticity. Despite their somehow artificial character, these simplified models enable one to focus on very basic mixing mechanisms and are particularly appropriate for investigating individual processes such as the relatively small-scale frontal mixing discussed in the present study.

The paper B91 represents a first attempt at understanding mixing in a two-dimensional eastward propagating meandering jet, showing that the exchange is due to the time-dependent propagation of the meanders, which causes fluid particles to cross streamlines.

The large-scale flow proposed in B91 has been utilized as a background field in further works where mixing is separately enhanced by two different transport mechanisms. S92 considers a modification of the B91 flow field where fluid exchange is induced by chaotic advection generated by a flow time dependence. The basic flow is made time dependent in three different fashions: the superposition of a time-dependent meridional velocity, that of a propagating plane wave and a time oscillation of the meander amplitude, which is the case we further investigate in this paper.

The Melnikov method (Lichtenberg and Lieberman 1992, LL92 hereafter) is used in S92 to explore the chaotic behavior around the separatrices of the original B91 flow when time dependence is added. One of the results of this investigation is that while mixing occurs between adjacent regions, over a broad range of the meander oscillation frequencies, it does not easily take place across the jet, that is, from recirculations south of the jet to recirculations north of it. This is inherently due to the oscillation pattern of the large-scale velocity, and we will discuss this in further detail in this paper.

Particle exchange in the same B91 flow is achieved by DGO93 by superimposing to the original time-independent basic flow a stochastic term that describes mesoscale turbulent diffusion in the upper ocean. The focus of that paper is on the exchange among recirculations and the jet core and vice versa, and on the homogenization processes in the recirculation. The numerical experiments presented in DGO93 are carried out for quite short integration times, which do not allow for exploring the mixing across the jet.

Since in the real ocean the two above mixing mechanisms, that is, chaotic advection and turbulent diffusion, are simultaneously present, in this paper we investigate how particle exchange varies through the progression from periodic to stochastic disturbances, revisiting and putting together the mixing processes studied by S92 and DGO93.

This is done by looking at particle statistics obtained by numerical computation of the trajectories of a large number of particles (or equivalently, since our system is ergodic, following one particle for a very long time) in three different flows: one equivalent to S92, in which mixing is induced by chaotic advection; one equivalent to DGO93, where it is due to turbulent diffusion; and a combination of them.

Dispersion processes in a flow field can be quantitatively characterized, in the Lagrangian description, in terms of different quantities, such as the Lyapunov exponent λ (Benettin et al. 1980) and the diffusion coefficients D_{ij} (LL92).

However the above indicators, even if mathematically well defined, can be rather irrelevant for many purposes. The Lyapunov exponent is the inverse of a characteristic

time t_L, related to the exponential growth of the distance between two trajectories initially very close together; however, other characteristic timescales may appear and result just as relevantly in the description of a system, such as those involved in the correlation functions and in the mixing phenomena. It is worth stressing that there is not a clear relationship, if any, among these times and t_L.

Also, the use of the diffusion coefficients can have severe limitations; sometimes the D_{ij} are not able to take into account the basic mechanisms of the spreading and mixing (Artale et al. 1997). Our western boundary current extension system has essentially a periodic structure in the zonal direction. It is thus possible to define and (numerically) compute the diffusion coefficients. They are related to the asymptotic behavior of a cloud of tracer particles. On the other hand, if one is interested in the meridional mixing, which takes place over finite timescales, the diffusion coefficients may not be very useful. In such situations it is then worthwhile to look for alternative methods of describing mixing processes, as was done by Artale et al. (1997) looking at dispersion in closed basins; by Buffoni et al. (1997), who employ exit times for the characterization of transport in basins with complicated geometry; or del Castillo-Negrete (1998), who studies the transport in terms of duration of flight probability distribution.

Our investigation is carried out with a nonconventional approach and in a geophysical contest as we try to analyze the system from the standpoint of the approximation in terms of Markovian processes (Fraedrich and Müller 1983; Fraedrich 1988; Kluiving et al. 1992; Cecconi and Vulpiani 1995; Nicolis et al. 1997).

We start from the consideration that the flow field, to be characterized in terms of fluid transport, can be subdivided into regions corresponding to different Lagrangian behavior: ballistic flight in the meandering jet core, trapping inside recirculations, and retrograde motion in the far field. As an obvious consequence, we introduce a partition of the two-dimensional physical space accessible to fluid particles and divide it into these disjoint regions selected in a natural way by the dynamics. At this point, the transition of fluid particles between different regions can be studied as a discrete stochastic process generated by the dynamics itself.

In this paper we study the statistical properties of this stochastic process and compare it with an approximation in terms of Markov chains. For some fluid exchange properties—such as the probability distribution of the particle exit times from the jet or from the neighboring recirculation regions—the effects of the two different mixing mechanisms and the results of the Markovian approximation are very similar. Other properties, such as the meridional mixing across the jet, do not show such an obvious possibility to be described in terms of Markovian simple processes. However, for those properties the Markovian description is seen to be relatively more accurate in the case when chaotic advection and turbulent diffusion are simultaneously present. The comparison between the results of the numerical simulations and those computed in the Markovian approximation allows for a deeper understanding of the transport and mixing mechanisms.

In section 2 we introduce the kinematic model for the field correspondent to the Gulf Stream flow and both models for chaotic advection and turbulent diffusion. Section 3 is devoted to the description of the Markovian approximation. In section 4 we discuss the numerical results and the comparison of the dynamics shown by the simulations with the Markovian approximation. Section 5 contains some discussion and conclusions. The appendix summarizes some basic properties of Markov chains.

2. The flow field

The large-scale flow in its basic form, representing the velocity field in correspondence of a meandering jet, is the same introduced in B91 and further discussed in S92; in a fixed reference frame the streamfunction is given by

$$\psi(x', y', t) = \psi_0 \left[1 - \tanh \frac{y' - A \cos\kappa(x' - c_x t)}{\lambda(1 + k^2 A^2 \sin^2\kappa(x' - c_x t))^{1/2}} \right],$$
(1)

where ψ_0 represents half of the total transport and A, k, and c_x are the amplitude, wavenumber, and phase speed of the pattern, respectively. A change of coordinates into a reference frame moving eastward with a velocity coinciding with the phase speed c_x, and a successive nondimensionalization, yield a streamfunction as follows:

$$\phi = -\tanh \left[\frac{y - B \cos kx}{(1 + k^2 B^2 \sin^2 kx)^{1/2}} \right] + cy.$$
(2)

The relationship between variables in (1) and (2) is given by (see S92)

$$x \equiv \frac{x' - c_x t}{\lambda}, \qquad y \equiv y'/\lambda, \qquad B \equiv A/\lambda$$

$$\phi \equiv \frac{\psi}{\psi_0} + cy, \qquad c \equiv \frac{c_x L}{\psi_0}, \qquad \kappa \equiv k\lambda.$$

The natural distance unit for our system is given by the jet width λ, here set to 40 km (B91, S92). The basic flow configuration is very similar to case (b) of B91: B was chosen as 1.2, c as 0.12. The only major difference is the value assigned to L, that is, the meander wavelength, which was set as 7.5, as will be discussed below.

The evolution of the tracer particles is given by

$$\frac{dx}{dt} = -\frac{\partial \phi}{\partial y}, \qquad \frac{dy}{dt} = \frac{\partial \phi}{\partial x}.$$
(3)

In Fig. 1 we show the stationary velocity vector field in the moving frame: the field is evidently divided into

three very different flow regions (see also B91, S92, DGO93): the central, eastward moving, jet stream; recirculation regions north and south of it; and a far field. The far field, given our choice of parameters, appears to be moving westward at a phase speed of $c_x \equiv -0.12$. This intrinsic self-subdivision of the flow field is crucial for building a partition of the possible states available to fluid particles, which will be investigated in Markovian terms.

Chaotic advection may be induced in a two-dimensional flow field by introducing a time dependence (e.g., Crisanti et al. 1991). This is simply achieved by adding to the basic steady flow some typically small perturbation that varies in time. Among three basic mechanisms discussed by S92, we chose here a time-dependent oscillation of the meander amplitude:

$$B(t) = B_0 + \epsilon \cos(\omega t + \theta). \qquad (4)$$

In (4) we set $B_0 = 1.2$, $\epsilon = 0.3$, $\omega = 0.4$, and $\theta = \pi/2$. These choices, as well as that for L, are motivated mainly by the results of observations by Kontoyiannis and Watts (1994) and of numerical simulations by Dimas and Triantafylou (1995). Namely, the most unstable waves produced in the latter work compare very well with the observations of the former, which show wavelengths of 260 km, periods of ~8 days, and e-folding time and space scales of 3 days and 250 km. In our case, since the downstream speed was set to 1 m s⁻¹, our e-folding timescale would correspond, in dimensional units, to approximately 3 days. The flow field resulting from the time-dependent version of (2) is shown in Fig. 2 for three subsequent time snapshots $t = T/4$ (Fig. 2a), $t = T/2$ (Fig. 2b), and $t = 3T/4$ (Fig. 2c), where $T = 2\pi/\omega$ is the period of the perturbation. Our system shows two different separatrices with a spatial periodic structure (see Fig. 2) north and south of the jet. At small ϵ one has chaotic motion around them but without meridional mixing. In order to have a "large-scale chaos," that is, the possibility that a particle passes from north to south (and vice versa) crossing the jet, one needs the *overlapping* of the *resonances* (Chirikov 1979) $\epsilon > \epsilon_c$. In our case, indeed $\epsilon > \epsilon_c$ and ϵ_c depends on ω (in Fig. 3 we show ϵ_c vs ω for our system).

The physical reason to have a "strong exchange" regime is that, for small values of the perturbation amplitude, the system would have stability isles inside the domain, for example, the cores of the gyres, from which particles would never escape unless in the presence of additional diffusive mechanisms. Since the mechanism we want to mimic, that is, the exchange in absence of ring detachment, has on the opposite a quite pervasive effect over the recirculation regions, in the framework of deterministic chaotic mixing this can be at least qualitatively reproduced just in a strong exchange regime.

The Lagrangian motion of a fluid particle is formally a Hamiltonian system whose Hamiltonian is the streamfunction ϕ. If $\phi = \phi_0(x, y) + \delta\phi(x, y, t)$, where

$\delta\phi(x, y, t) = O(\epsilon)$ is a periodic function of t, there exists a well-known technique, due to Poincaré and Melnikov, which allows one to prove whether the motion is chaotic (LL92). Basically if the steady part $\phi_0(x, y)$ of the streamfunction admits homoclinic (or heteroclinic) orbits, that is, bounding streamlines on which one has a periodic motion with infinite period (the separatrices), then the motion is usually chaotic in a small region around the separatrices for small values of ϵ.

In S92 the Melnikov method has been explicitly used for the ϕ_0 and $\delta\phi$ that we have used in this paper, and thus proved, in a rigorous way, the existence of Lagrangian chaos. However, even if the Melnikov method can determine if the Lagrangian motion is chaotic, it may not be suitable for the study of other interesting properties, which will be the focus of section 4a.

Alternatively (or jointly), mixing in the flow field (2) can be created by adding a turbulent diffusion term. This was done using a stochastic model for particle motion belonging to the category of the so-called random flight models (e.g., Thomson 1987), which can be seen as simple examples of a more general class of stochastic models that can be nonlinear and have arbitrary dimensions, described by the generalized Langevin equations (Risken 1989; for a review, see Pope 1994):

$$ds_i = h_i(\mathbf{s}, t) \, dt + g_{i,j}(\mathbf{s}, t) \, d\mu_j, \qquad i = 1, \cdots, N, \quad (5)$$

where $\mathbf{s} = (s_1, \ldots, s_N)$ are N stochastic variables, which, in our context, are the turbulent velocity fluctuations, μ_i is a random process with independent increments, and h_i and $g_{i,j}$ are continuous functions. A general, remarkable characteristic of these models is their Markovian nature, which obviously has a particular interest for this investigation. The theoretical motivation for the choice of Markovian models to describe mesoscale ocean turbulence has been thoroughly discussed in Zambianchi and Griffa (1994a), Griffa (1996), and Lacorata et al. (1996); it is worth adding that this particular model has proved to accurately represent upper-ocean turbulence in regions characterized by homogeneity and stationarity [see Colin de Verdière (1983), Zambianchi and Griffa (1994b), Griffa et al. (1995), Bauer et al. (1998), but also the results of numerical simulations by Verron and Nguyen (1989), Yeung and Pope (1989), Davis (1991)], and is easily extended to more complex situations (van Dop et al. 1985; Thomson 1986).

In our simulations, a turbulent velocity $\delta\mathbf{u}^{(T)}(\mathbf{x}, t)$ is added to the large-scale velocity field $\mathbf{u}^{(M)}(\mathbf{x}, t)$ resulting from the streamfunction (2). The resulting equation for the particle trajectory is

$$\frac{d\mathbf{x}}{dt} = \mathbf{u}(\mathbf{x}, t), \qquad (6)$$

where $\mathbf{u}(\mathbf{x}, t)$ is given by

$$\mathbf{u}(\mathbf{x}, t) = \mathbf{u}^{(M)}(\mathbf{x}, t) + \delta\mathbf{u}^{(T)}(\mathbf{x}, t). \qquad (7)$$
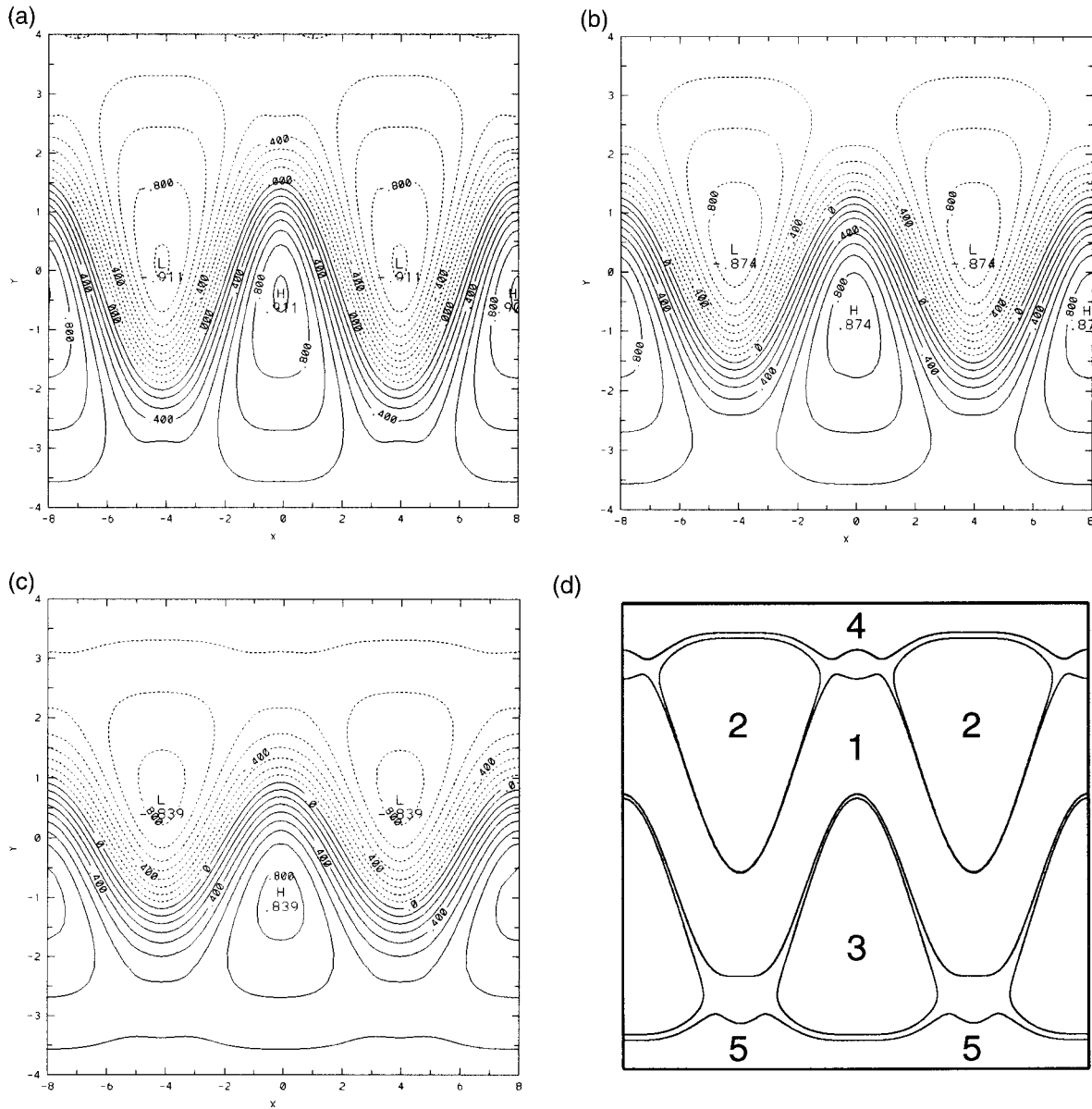
FIG. 2. Streamlines of the time-dependent streamfunction (2), with B given by Eq. (4), $B_0 = 1.2$, $\omega = 0.4$, and $\epsilon = 0.3$ ($T = 2\pi/\omega$), at three different times: (a) $t = T/4$, (b) $t = T/2$, and (c) $t = 3T/4$. In (d) the partition is shown.

Our model assumes $\delta\mathbf{u}^{(T)}(\mathbf{x}, t) = \delta\mathbf{u}^{(T)}(t)$ as a Gaussian process with zero mean and correlation:

$$\langle \delta u_i^{(T)}(t) \delta u_j^{(T)}(t') \rangle = 2\sigma^2 \delta_{ij} e^{-|t-t'|/\tau}. \qquad (8)$$

With this choice, $\delta\mathbf{u}^{(T)}(t)$ is a Markovian process linear in time. The turbulent field is entirely described in terms of two parameters: the variance of the small-scale velocity σ^2 and the e-folding timescale of the velocity autocorrelation function, that is, its typical correlation timescale τ. In absence of the large-scale velocity the diffusion coefficient is $\sigma^2\tau$. The interdependence among smaller and larger timescales of the Lagrangian motion will be investigated in the following chapters.

3. The Markovian approximation

a. Generalities

The idea of using stochastic processes to investigate chaotic behavior is fairly old (Chirikov 1979; Benettin 1984). One of the most relevant and successful approaches is symbolic dynamics, which allow one to give a detailed description of the statistical properties of a chaotic system in terms of a suitable discrete stochastic process (Beck and Schlögl 1993).

Given a discrete dynamical system:

$$\mathbf{x}_t = S^t\mathbf{x}_0, \qquad (9)$$
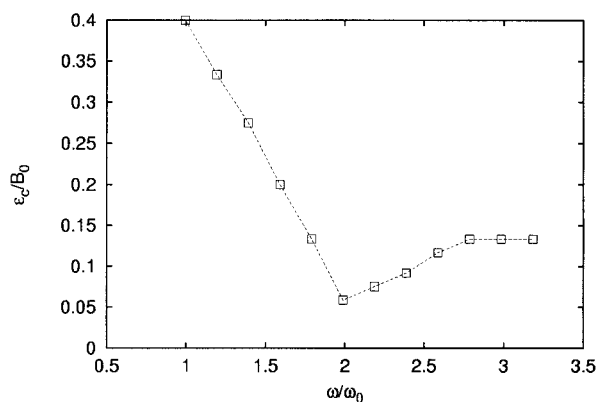
FIG. 3. Critical values of the periodic perturbation amplitude for the overlap of the resonances, ϵ_c/B_0 vs ω/ω_0, for the streamfunction (2) with $L = 7.5$, $B_0 = 1.2$, $c = 0.12$, and $\omega_0 = 0.25$, which is the typical frequency for the rotation of a tracer particle along the boundary of the recirculating gyres. The critical values have been estimated following a cloud of 100 particles initially located between the states 1 and 2 for 500 periods.

a partition $\mathcal{A}$ can be introduced, dividing the phase space in A_1, A_2, ..., A_N disjoint sets, or cells (with $A_i \cap A_j = 0$ if $i \neq j$). Given a trajectory

$$\mathbf{x}_0, \mathbf{x}_1, \ldots, \mathbf{x}_n, \ldots. \tag{10}$$

The point $\mathbf{x}_0 \in A_{i_0}$ is put in correspondence with the integer i_0, the next one $\mathbf{x}_1 \in A_{i_1}$ the integer i_1 and so on. Therefore any initial condition $\mathbf{x}_0$ determines a certain symbol sequence:

$$\mathbf{x}_0 \rightarrow (i_0, i_1, \ldots, i_n, \ldots). \tag{11}$$

Now the study of the *coarse grained* properties of the chaotic trajectories is reduced to the statistical features of the discrete stochastic process $(i_0, i_1, \ldots, i_n, \ldots)$. A useful and important characterization of the properties of symbolic sequences is the Kolmogorov–Sinai entropy, which measures the time rate of loss of information as a trajectory evolves (Eckmann and Ruelle 1985; Badii and Politi 1997), defined by

$$h_{\mathrm{KS}} = \lim_{n \to \infty} (H_{n+1} - H_n), \tag{12}$$

with

$$H_n = \sup_{\{\mathcal{A}\}} \left[-\sum_{C_n} P(C_n) \ln P(C_n) \right] \tag{13}$$

and

$$C_n = (i_0, i_1, \ldots, i_{n-1}), \tag{14}$$

where $P(C_n)$ is the probability of the sequence C_n and $\{\mathcal{A}\}$ is the set of all possible partitions. The quantity $H_{n+1} - H_n$ represents the additional averaged information needed to specify the symbol i_{n+1} given the previous i_n (Badii and Politi 1997).

Notice that, from a theoretical point of view, the sup in (13) hides a very subtle point: there sometimes exists

a particular partition, called *generating partition,* from which the sup is directly obtained. A partition is generating if the infinite symbol sequence i_0, i_1, ..., i_n, ... uniquely determines the initial value $\mathbf{x}_0$.

However, assessing the possible existence of a generating partition for a given system may be nontrivial; furthermore, from a practical point of view, even if a system is known to admit a generating partition, determining it may be a very hard task (see Beck and Schlögl 1993, for more details).

The stochastic process given by the symbol dynamics with a given partition can have rather nontrivial features. Of course the optimal case is when the symbolic stochastic process is a Markov chain; that is, the probability to be in the cell A_i at time t depends only on the cell at time $t - 1$. In this case it is possible to derive all the statistical properties (e.g., entropy and correlation functions) from the transition matrix W_{ij} whose elements are the probabilities to find the system in the cell A_j at time t if at time $t - 1$ the system is in the cell A_i. See the appendix for a summary of the properties of Markov chains.

An accurate description of a chaotic system typically requires a higher-order Markovian process, that is, one in which the probability for the system to be in the cell A_j at time t depends on more previous steps (we have a k-order process, e.g., when the probability to be in the cell A_j at time t depends only on the preceding k steps $t - 1, t - 2, \ldots, t - k$). In particular it is possible to estimate the order of the Markov process necessary to reproduce the statistics of the process $(i_0, i_1, \ldots, i_n, \ldots)$ generated by the dynamics by means of the quantities defined in Eqs. (12) and (13) and on the basis of considerations drawn from information theory (see Khinchin 1957). It can be shown (Khinchin 1957) that, defining

$$h_n = H_n - H_{n-1} \tag{15}$$

with H_{n-1} given by (13), if the process is a Markov process of order k then $h_n = h_{\mathrm{KS}}$ for $n \geq k + 1$. In the next section we will apply this method to give an estimate of the order k for our system.

Typically, using a Markovian approximation of order $k \leq 5$, it is relatively easy to find a reasonable agreement with the observed K–S entropy (12), or the Lyapunov exponent. On the other hand, correlation functions and other observables can be just roughly caught by even quite higher order Markov processes ($k \simeq 10$).

Mimicking a low-dimensional dynamical system in terms of higher-order Markov processes represents an interesting issue in the field of chaotic dynamics but has, in our opinion, just a weak relevance for many practical purposes in geophysics since very large statistics are needed for the computation of the transition probabilities. Therefore we shall restrict our analysis to the simplest case of the approximation in terms of a Markov chain, that is, of a first-order process. This practical approach has been successfully used in the study

of the dynamical properties of small astronomical bodies such as comets (see Rickmann and Froeschlé 1979; Levinson 1991) and for the interpretation of atmospheric phenomena (Fraedrich 1988; Fraedrich and Müller 1983).

b. The present application

In this section we explain how we expressed the behavior of our Gulf Stream–like system in terms of symbolic dynamics. First we reduced the ordinary differential equation (3) obtained by the streamfunction (2) to a dynamical system discrete in time. This was accomplished building the Poincaré map associated with (3). The aim of this method is to write a stroboscopic map connecting the value of $\mathbf{x}$ at time $t = nT$ with those at $t = (n + 1)T$, that is, to write $\mathbf{x}_{n+1}$ in terms of $\mathbf{x}_n$ [where $\mathbf{x}_n = \mathbf{x}(t = nT)$]:

$$\mathbf{x}_{n+1} = \mathbf{F}[\mathbf{x}_n]; \qquad (16)$$

it is worth underlining the importance of the existence of such a relationship, even if in general writing down an explicit expression for $\mathbf{F}[\mathbf{x}_n]$ may be nontrivial.

As discussed above, a crucial point is represented by the suitable choice of a phase space partition. Considering the streamline pattern of our flow field (Fig. 2), the structure of the physical space accessible to fluid particles suggests an obvious, natural choice for the partition: a particle will find itself in state 1 when it is inside the jet core (open trajectories); states 2 and 3 correspond to trapping in the northern and southern recirculations, respectively (closed trajectories), and states 4 and 5 to the far field (backward open trajectories).

This partition, see Fig. 2d, turns out to be particularly appropriate to describe some important mixing properties of our system, such as

(a) the residence time of particles in the trapping recirculations or inside the jet, which in the language of Markov chain (see appendix) correspond to the first exit time from state i ($i = 1, \ldots, 5$);
(b) the meridional mixing time (MMT), that is, the time it takes a particle to enter the northern (southern) recirculation starting from the southern (northern) one, that is, the time of first passage from cell 2 (3) to cell 3 (2);
(c) the correlation function for a variable $\chi_i(n)$, which indicates if a determined state i is visited at time n [see below, Eqs. (23) and (24), and appendix].

Let us now describe how to compute statistics for the quantities (a, b, c). First of all, from a long trajectory $\mathbf{x}_0, \mathbf{x}_1, \ldots, \mathbf{x}_n$ ($n \gg 1$) we can compute the transition probabilities:

$$W_{ij} = \lim_{n \to \infty} \frac{N_n(i, j)}{N_n(i)}, \qquad (17)$$

where $N_n(i)$ is the number of times that, along the trajectory, $\mathbf{x}_t$ ($t < n$) visits the cell A_i and $N_n(i, j)$ is the number of times that $\mathbf{x}_t \in A_i$ and $\mathbf{x}_{t+1} \in A_j$.

Notice that, for each i

$$\sum_j W_{ij} = 1 \qquad (18)$$

and because of the system symmetries, states 2 and 3 possess the same statistical properties and so do states 4 and 5; in particular, the following equalities hold:

$$W_{12} = W_{13}, \qquad W_{23} = W_{32},$$
$$W_{21} = W_{31}, \qquad W_{22} = W_{33}, \quad \text{and so on.} \qquad (19)$$

We can express the visit probabilities $\{P_i\}$ (i.e., the probability to be in the state i) in terms of the matrix $\{W_{ij}\}$ as follows:

$$P_i = \sum_j P_j W_{ji}. \qquad (20)$$

Let us stress that Eqs. (18) and (20) hold even if the process is not a Markov chain.

Under the assumption (approximation) that the symbolic stochastic process generated by our deterministic chaotic model is a Markov chain, one can derive (see appendix) the probability $[P_i(n)]$ of the first exit times from state i in n steps:

$$P_i(n) = \left[\frac{(1 - W_{ii})}{W_{ii}}\right](W_{ii})^n, \qquad (21)$$

which is the statistics of residence times in state i. A slightly more complicated computation gives the probabilities $f_{ij}(n)$ of first passage from state i to state j in n steps:

$$f_{ij}(n) = (W^n)_{ij} - \sum_{k=1}^{n-1} f_{ij}(n - k)(W^k)_{jj}, \qquad (22)$$

where W^k indicates the kth power of the matrix W. For the normalized correlation function $C_i(n)$ of the variable $\chi_i(n)$, defined as

$$\chi_i(n) = \begin{cases} 1, & \text{if } \mathbf{x}_n \in A_i \\ 0, & \text{otherwise,} \end{cases} \qquad (23)$$

we have

$$C_i(n) = [(W^n)_{ii} - P_i]/(1 - P_i). \qquad (24)$$

The Kolmogorov–Sinai entropy for the Markov chain is nothing but the Shannon entropy for a Markov chain (Khinchin 1957):

$$h_{KS} = h_S = - \sum_{i,j} P_i W_{ij} \ln W_{ij}. \qquad (25)$$

Notice that for a Markov process $h_n = H_n - H_{n-1} = h_{KS}$ for $n = 2$ (see above). Since the discrete time system is obtained observing it at times $0, T, 2T, \ldots$, the Lyapunov exponent λ of the original system has to be compared with

$$\lambda_M = \frac{h_S}{T}. \tag{26}$$

This last equation is easily understood by noticing that h_{KS} gives the degree of information per step produced by the process, which, apart from a time rescaling, for a chaotic system in two dimensions corresponds to the Lyapunov exponent.

Meiss and Ott (1986) and Mackay et al. (1987) proposed a Markov model for transport in two-dimensional area preserving maps (corresponding to Lagrangian motion in a two-dimensional time-periodic incompressible velocity field). This approach, very interesting from a dynamical systems point of view, involves a fairly complex subdivision of the phase space, which makes its adoption quite hard for the study of realistic flows and analysis of data. In particular, it implies the necessity of having a complete partition of the phase space into stochastic subregions where all orbits have an infinite Lyapunov exponent [these aspects are thoroughly discussed in chapter 5 of Wiggins (1992)]. In practical terms, this translates into building a partition made up by a very large number of cells, which goes in the opposite direction of the simplified but practical method proposed in this paper, which uses a partition defined by relatively large-scale properties of the flow dynamics.

4. Numerical results

We now discuss the numerical results for the models introduced in section 2 and their comparison with the Markovian approximation illustrated in section 3.

a. Mixing induced by chaotic advection

We first consider the deterministic model with the parameter B of the streamfunction Eq. (2) varying periodically in time according to Eq. (4) with the parameters $B_0 = 1.2$, $\epsilon = 0.3$, $\omega = 0.4$, $\phi = \pi/2$, and $c = 0.12$ (see section 2). With this choice the system is chaotic and exhibits mixing at large scale, that is, north–south mixing occurs.

We show in Fig. 4 the spreading at different times of a cloud of tracer particles. The domain is naturally defined from the basic cell that repeats itself creating a zonal periodic structure of wavelength L; x thus varies in $[0, L]$, while y in $[-4, 4]$. We fixed a posteriori these bounds for y since for our choice of parameters no particles reach the far field, and no trajectory attains values in $|y|$ larger than 4 (even though, in general, we expect low but nonzero frequencies for these states, see also S92).

In general, whether a north–south mixing happens or not depends sensibly on the values of ϵ and ω. Typically the system reveals a strong preference to have long residence times in the northern or the southern half of the domain with respect to the jet core. This peculiar feature

will play an important role in the comparison with the Markovian approximation.

The transition matrix elements W_{ij} and the visit probabilities $\{P_i\}$ were computed by means of Eq. (17), looking at **x** every period, that is, for $t = T, 2T, \ldots$, where $T = 2\pi/\omega$, and the estimated values are reported in Tables 1 and 2. At a first glance, we can see that the requested symmetry properties are respected [Eq. (19)].

In order to test whether the system is well approximated by a first-order Markov process we computed exit times, correlation functions, meridional mixing times, and Lyapunov exponent from the simulations and compared them with the Markovian predictions.

In Fig. 5 we show the first exit time probability distributions for the states 1 and 2 (3) and the corresponding Markovian predictions. After underlining that the straight lines of Fig. 5 are not to be confused with best-fit curves, we see that the agreement is good over a certain range both for states 1 and 2 (3). The agreement between the Markovian predictions and the simulation results is rather poor for small and very large exit times. This behavior shows that the Markovian approximation cannot hold at small times since the details of the dynamics are strongly relevant. In the same way nontrivial long time correlations cannot be accounted for in terms of a first-order Markovian process.

In Fig. 6 we can see how the correlation functions of χ_i [see Eqs. (23)–(24)] for states 1 and 2 (3) are just in vague agreement with the corresponding correlations obtained for the Markovian process. The trajectories in the recirculations (i.e., states 2 and 3) appear to be much more autocorrelated than those in the jet. Therefore we deduce that the system, although chaotic, has a strong memory as to which half (northern or southern) of the spatial domain it is visiting. The typical evolution is a "rebound game" between state 2 and the southern half of the jet during a certain time interval; then it crosses the jet core and performs again the same pattern between state 3 and the northern half of the jet, until it jumps back, and so on. This is strikingly evident if we look at the distribution probabilities of the meridional mixing times, where the Markovian approximation completely fails (Fig. 7).

This can be explained as follows: the simulations show that, when a tracer particle leaves a recirculation region, say in the southern half, and enters the jet, most of the time it returns back to some other close orbit in the southern half of the basin rather than crossing the jet barrier, showing a long memory effect, which is not featured in the first-order Markov approximation. This is a clear indication that higher-order Markov processes are necessary to describe this portion of the statistics produced by the dynamics. This is shown in Fig. 8, where transitions between states 1 and 2, and 1 and 3, are compared: whereas in the first-order Markovian approximation (Fig. 8b) a particle jumps very often from north to south, the results of our numerical experiments show a stronger tendency for particles to keep being
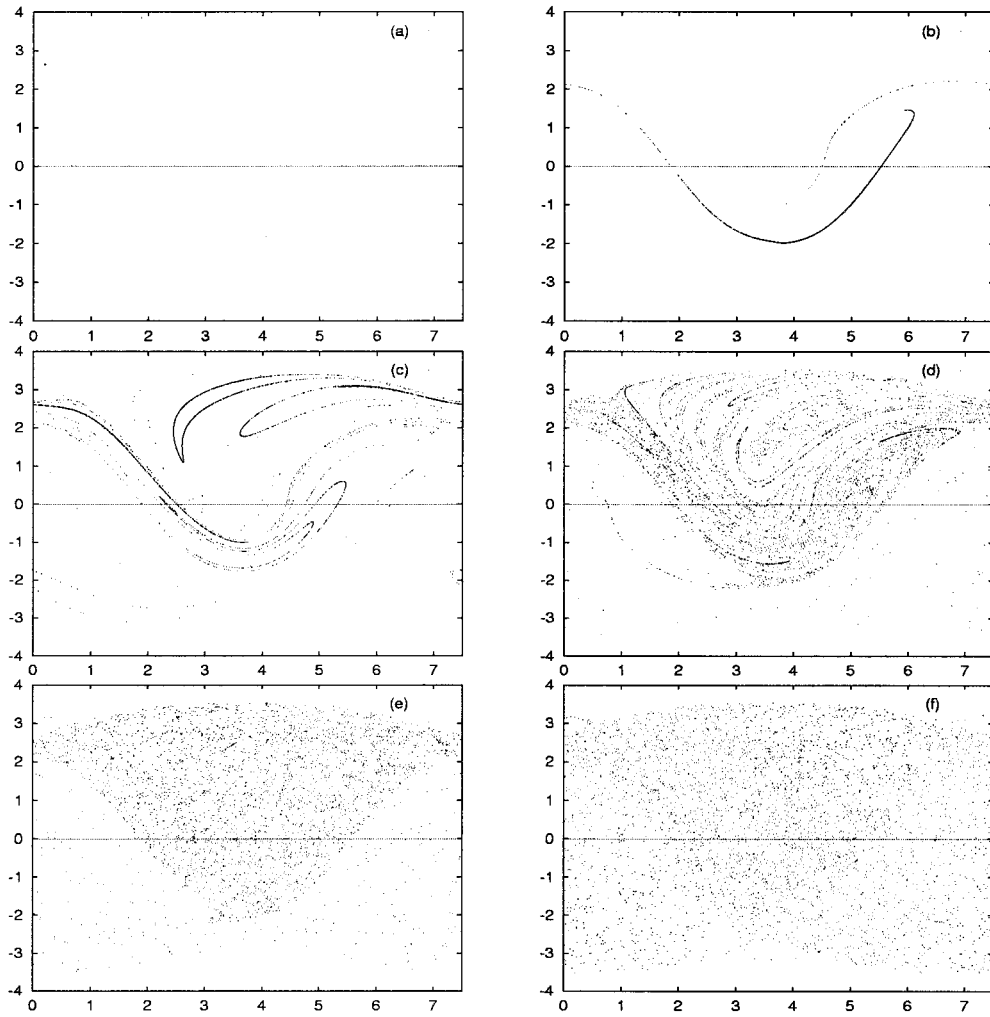
FIG. 4. Spreading of a cloud of 5000 particles at different times for the deterministic model (see Fig. 2) at (a) $t = 0$: the particles are initially located inside a 0.05 by 0.05 square centered in (0.1, 2.7), (b) $t = T$, (c) $t = 5T$, (d) $t = 10T$, (e) $t = 20T$, and (f) $t = 100T$.

confined either between states 1 and 2 or between 1 and 3 (Fig. 8a).

To quantify the relevance of the memory effects we computed the block entropies h_n, defined in section 3 [Eq. (15)] at varying n. In Fig. 9 we can see that to obtain the convergence of the entropies we need at least a Markov approximation of order 6 or 7.

The Lyapunov exponent computed with a standard algorithm (see Benettin et al. 1980) is $\lambda = 0.05$, the first-order Markov approximation gives $\lambda_M = 0.03$, while the extrapolation with the asymptotic value $h = \lim_{n \to \infty} h_n$ gives $\tilde{\lambda}_M = 0.03$. That $\tilde{\lambda}_M < \lambda$ is probably due to the fact that the partition used here is not a generating one (see section 3); however, there exists a

TABLE 1. Transition matrix elements.

W_{ij}	Case A	Case B	Case C
W_{11}	0.66	0.74	0.58
W_{12}	0.17	0.13	0.21
W_{13}	0.17	0.13	0.21
W_{21}	0.12	0.09	0.14
W_{22}	0.88	0.91	0.86
W_{23}	0.00	0.00	0.00
W_{31}	0.12	0.09	0.14
W_{32}	0.00	0.00	0.00
W_{33}	0.88	0.91	0.86

TABLE 2. Visit probabilities for case A: deterministic chaotic model defined by Eq. (3) related to the streamfunction (2) with parameters $L = 7.5$, $B_0 = 1.2$, $c = 0.12$, $\omega = 0.4$, and $\epsilon = 0.3$; case B: turbulent diffusion model defined by Eqs. (27) and (28) with parameters $\sigma = 0.05$ and $\tau = T/4$; and case C: model with chaotic advection plus turbulent diffusion with the same parameters of case A and B. The statistics have been computed over 2×10^6 periods.

P_i	Case A	Case B	Case C
P_1	0.26	0.25	0.25
P_2	0.37	0.375	0.375
P_3	0.37	0.375	0.375
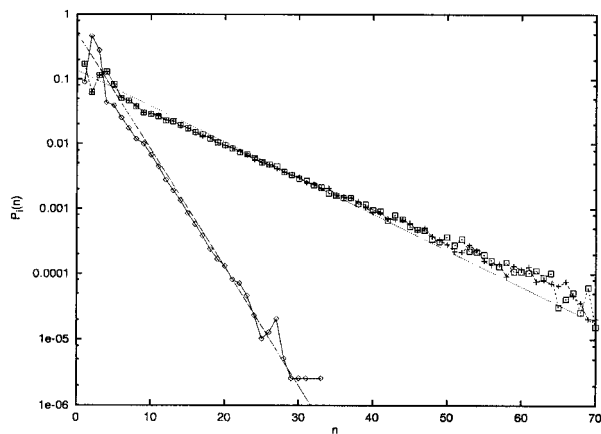
FIG. 5. Probability distribution of the first exit times from states 1 (diamonds), 2 (squares), and 3 (crosses) for the deterministic model (see Fig. 2). The straight lines are the Markovian predictions given by Eq. (A5) with W_{ii} of Table 1 (case A). The time unit is the period T of the perturbation. The statistics is computed over 2×10^6 periods.
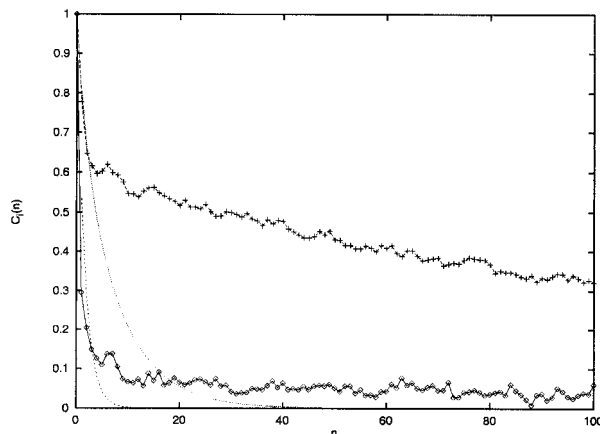
FIG. 6. Correlation functions of states 1 (diamonds) and 2 (crosses) compared with the Markovian predictions [continuous lines, Eq. (A11)] for the deterministic model (see Fig. 2).

fair agreement between $\tilde{\lambda}_M$ and λ. It is worth noticing that the above features are fairly robust and do not vary in a relevant way after weak changes of parameters.

b. Mixing induced by turbulent diffusion

The same investigation discussed in the previous subsection was carried out setting $\epsilon = 0$ and turning on turbulent diffusion, which is described in terms of a stochastic model for particle motion:

$$\frac{dx}{dt} = u + \eta_1, \qquad \frac{dy}{dt} = v + \eta_2, \qquad (27)$$

where u, v are given by the streamfunction (2) and η_i are zero-mean Gaussian stochastic processes with $\langle \eta_i(t)\eta_j(t') \rangle = \sigma^2 \delta_{ij} \exp(-|t - t'|/\tau)$. The Gaussian variable η_i is generated by a Langevin equation (Chandrasekhar 1943):

$$\frac{d\eta_i}{dt} = -\frac{\eta_i}{\tau} + \sqrt{\frac{2\sigma^2}{\tau}}\zeta_i, \qquad i = 1, 2, \qquad (28)$$

where the variables ζ_i are zero-mean Gaussian noises with $\langle \zeta_i(t)\zeta_j(t') \rangle = \delta_{ij}\delta(t - t')$. The numerical integration of the equations has been performed by means of a stochastic fourth-order Runge–Kutta algorithm (Mannella and Palleschi 1989).

Now the motion is unbounded for the presence of the isotropic diffusive terms; therefore, in order to get a transition matrix comparable with the matrix obtained in the chaotic deterministic case and to be able to compare the two models, we need to limit the dispersion along y inside a domain as similar as possible to the previous one.

Since the chaotic model does not fill states 4 and 5, we impose that, if a tracer enters a backward motion region, it is reflected back by changing the sign of the

meridional turbulent velocity. We emphasize that this boundary condition practically does not affect the mixing process between the jet and the recirculation regions.

In the diffusive case we set the values $\sigma = 0.05$ and $\tau = T/4$ as representative of an observable situation (see Okubo 1971) and compute again the transition matrix and stationary frequencies of the five states (see Tables 1 and 2). The elements of the transition matrix are close to those of the chaotic case. The transition probabilities were computed over a time period T as was done for the chaotic case so that the two cases can be compared.

In Fig. 10 we show the spreading of a cloud of particles. Figure 11 shows the probabilities of the first exit times of the states 1, 2, and 3 and the relative Markovian predictions. The distributions derived from the simulations are very well approximated by the first-order Markov process.

The correlation functions are shown in Fig. 12. The difference between the actual and the Markovian curves is now smaller than in the chaotic case because of the
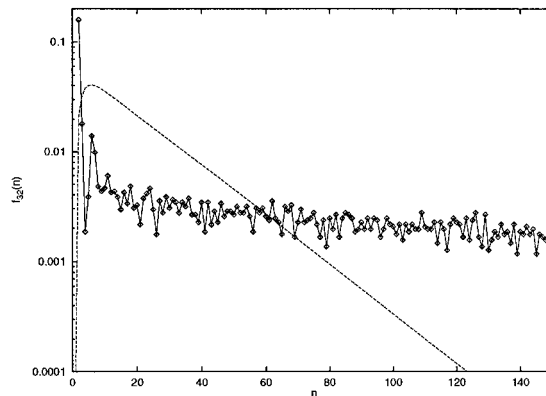
FIG. 7. Probability distribution of the meridonal mixing times (MMT) compared with the Markovian predictions [continuous lines, Eq. (A5)] for the deterministic model (see Fig. 2).
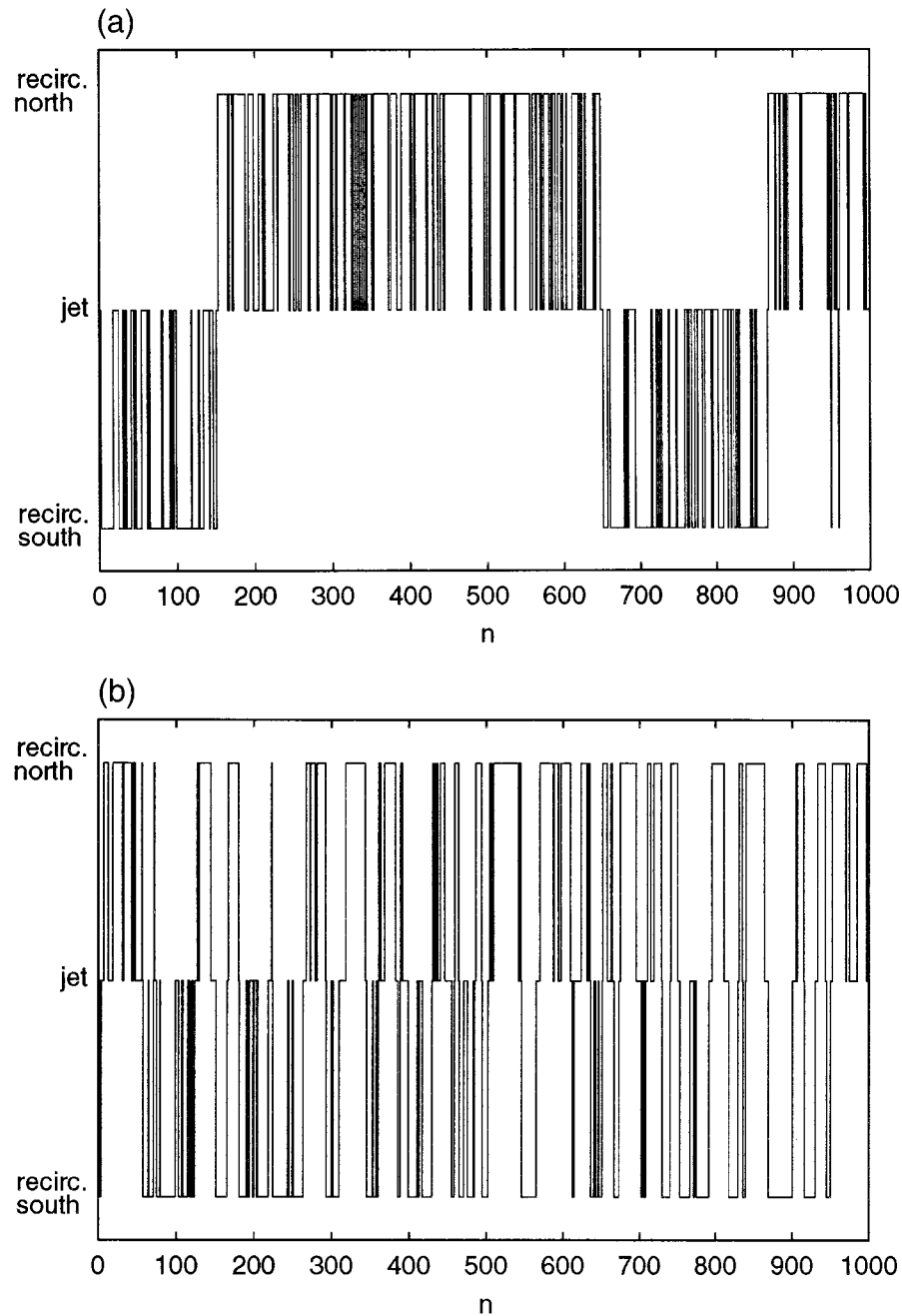
FIG. 8. Comparison between (a) the symbolic sequence of the states as function of time (for $t = T, 2T, \ldots$) obtained by the integration of the deterministic model [Eqs. (1) and (2)] and (b) the symbolic sequence generated from the Markov chain defined by the transition matrix computed as described in Eq. (17) and reported in Table 1 (case A).

presence of diffusion that decreases sensibly the degree of memory. This is much more evident looking at the distributions of the meridional mixing times (see Fig. 13).

Thus we can conclude that in the diffusive model the one-step Markovian approximation is much more appropriate than in the chaotic one. Looking at the block entropies h_n (15), we have a clear indication that the process is of a lower order with respect to the chaotic case (cf. Fig. 14 with Fig. 9).

Just like in the previous case we have investigated the behavior of the system, varying the parameters σ and τ. We have observed that, if we keep the quantity $\sigma^2\tau$ constant, the system displays a qualitatively constant behavior, even though the extent of the agreement between simulation results and Markovian approxima-
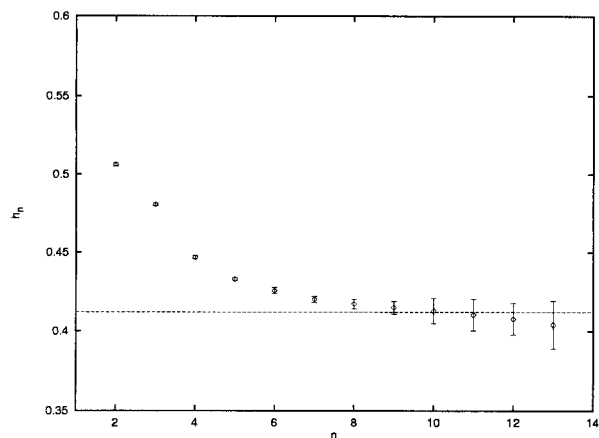
FIG. 9. Block entropies h_n vs n (15) for the deterministic model (see Fig. 2), computed from a sequence of 10^6 symbols.

tion slightly differs for different values of the turbulence parameters; this can be understood if we recognize that $\sigma^2\tau$ corresponds to the diffusion coefficient (see, e.g., Zambianchi and Griffa 1994a). It has been shown that varying σ and τ even though keeping the diffusion coefficient constant can indeed affect the quantitative estimates of dispersion in cases characterized by inhomogeneity and/or nonstationarity (see, again, Zambianchi and Griffa 1994a). On the other hand, the qualitative functional behavior of the dispersion processes has been seen to be affected very little by such changes in the parameters of turbulence (Lacorata et al. 1996).

c. Mixing jointly induced by chaotic advection and turbulent diffusion

A detailed analysis of Lagrangian data from the ocean aimed at determining contemporary presence and relative importance of chaotic and turbulent mixing is at
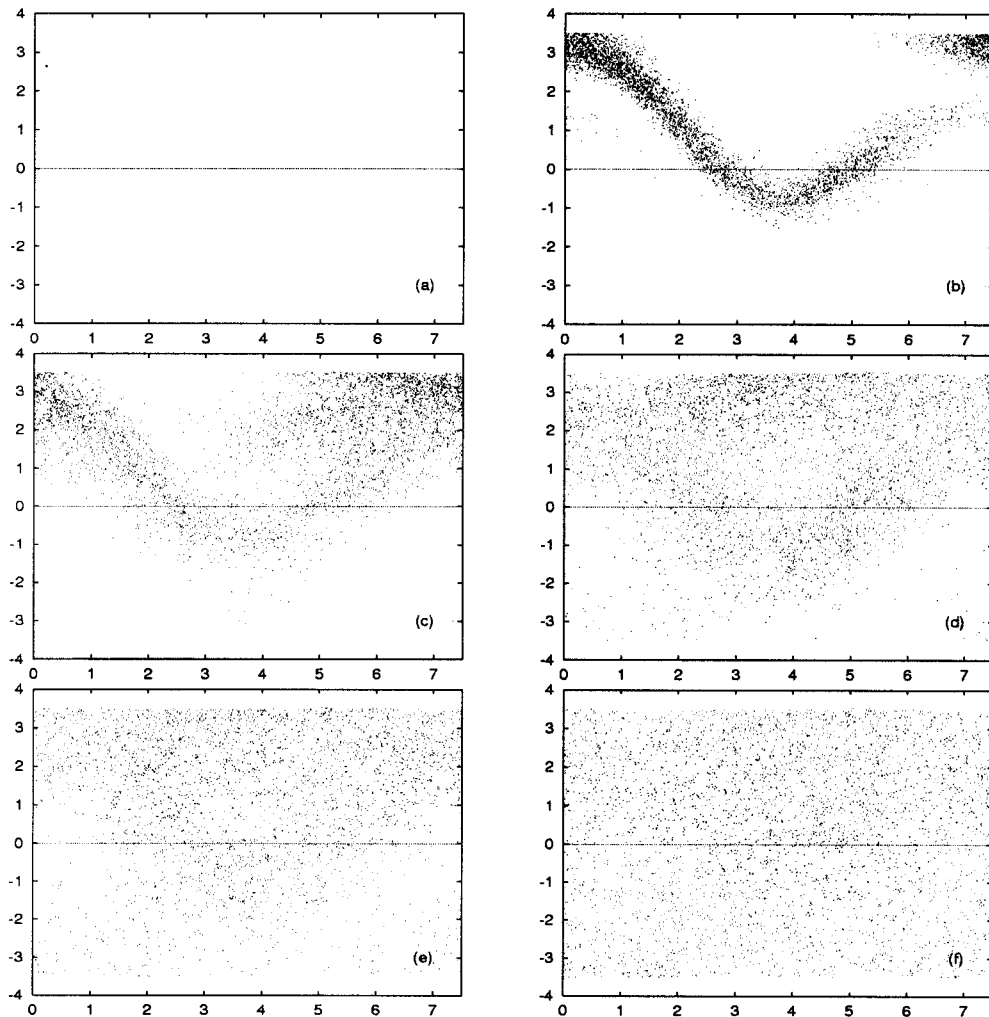
FIG. 10. Same as Fig. 4 but for the stochastic model given by Eqs. (27) and (28), with parameters $\sigma = 0.05$ and $\tau = T/4$. The time unit T is set equal to the period of the deterministic perturbation (see Fig. 2). The particles are initially located inside a 0.05 by 0.05 square centered in (0.1, 2.7).
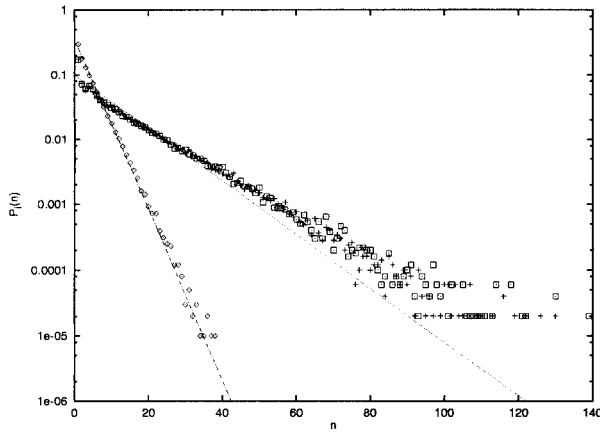
FIG. 11. Probability distribution of the first exit times from states 1, 2, and 3 for the stochastic model (see Fig. 10). The straight lines are the Markovian predictions given by Eq. (A5) with W_{ii} of Table 1 (case B).
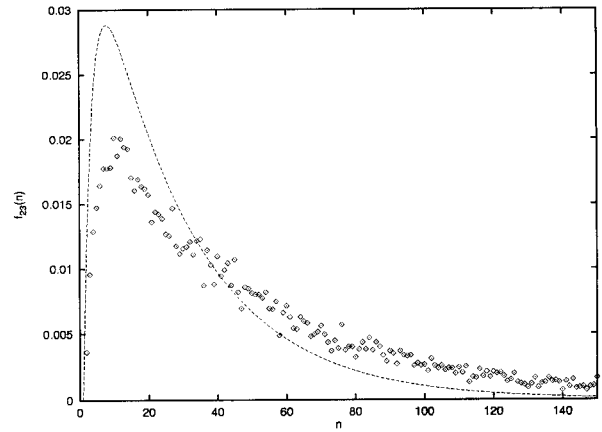
FIG. 13. Probability distribution of the MMTs compared with the Markovian predictions [Eq. (A7)] for the stochastic model (see Fig. 10).

present still lacking, as it would imply the evaluation of both one- and two-particle statistics parameters, which has been done only in the context of purely diffusive particle exchange investigations (see, e.g., Poulain and Niiler 1989). However, in the real ocean we expect both the above mixing mechanisms, discussed in section 2, to be present at the same time.

One of the interesting results of the previous sections is not only that we can look at particle exchange in terms of Markovian processes, but also that the sampling time suitable for the description of chaotic and turbulent exchange are of the same order of magnitude for fairly realistic simulations. This suggests the feasibility of a numerical experiment in which a stochastic term is added to a time-dependent large-scale velocity field.

In addition, in the introduction we mentioned the issue of a possible inconsistency of kinematic models as to the lack of Lagrangian conservation of quantities such

as potential vorticity. This difficulty, which has been recently discussed at length for two-dimensional chaotic flows (see, above all, Brown and Samelson 1994), is overcome in the combination of the two mixing processes, as turbulent diffusion can be seen as a sort of dissipation, which therefore acts so as to "smear" potential vorticity gradients.

In this numerical experiment we use the model equations (6) and (7) with $\mathbf{u}^{(M)}(\mathbf{x}, t)$ given by the streamfunction (2) with the time-dependent perturbation (4), and for the turbulent velocity $\delta\mathbf{u}^{(T)}(\mathbf{x}, t)$ we use the stochastic process defined in Eqs. (27)–(28); the parameters are $B_0 = 1.2$, $\epsilon = 0.3$, $\omega = 0.4$, $\theta = \pi/2$, $\sigma = 0.05$, and $\tau = T/4$ where $T = 2\pi/\omega$. As can be seen, this choice for the parameters is simply a superposition of the two previous cases.

Also in this case the matrix elements (i.e., the transition probabilities) are comparable with the other ones (see Table 1). As shown in Figs. 15 and 16, the distributions of the residence times and of the meridional
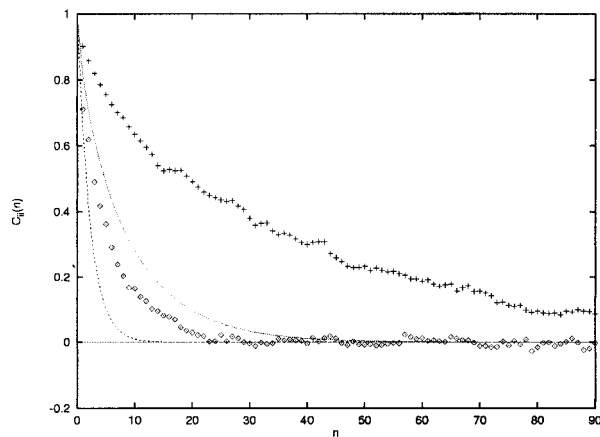
FIG. 12. Correlation functions compared with the Markovian predictions [continuous lines, from Eq. (A11)] for the stochastic model (see Fig. 10).
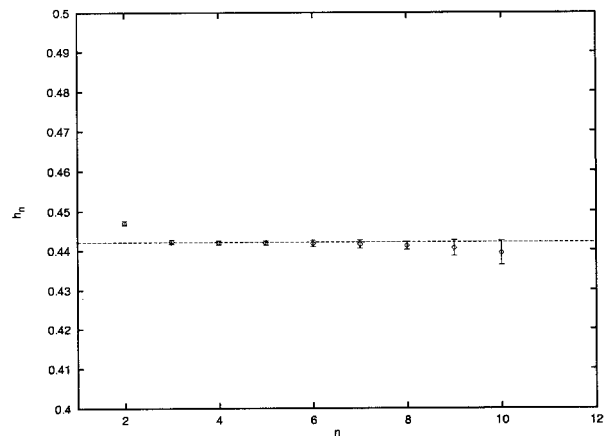
FIG. 14. Block entropies h_n vs n for the stochastic model, computed from a sequence of 10^6 symbols.
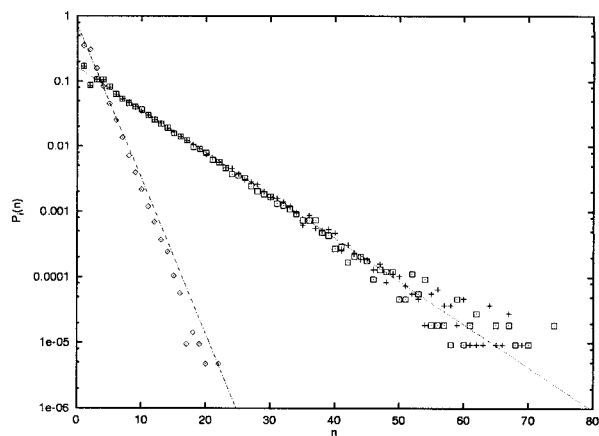
FIG. 15. Probability distributions of the first exit times from states 1, 2, and 3 in the model with chaotic advection combined with turbulent diffusion with parameters: $B_0 = 1.2$, $\omega = 0.4$, $\epsilon = 0.3$, and $\sigma = 0.05$, $\tau = T/4$ where $T = 2\pi/\omega$. The straight lines are the Markovian predictions given by Eq. (A5) with W_{ii} of Table 1 (case C).
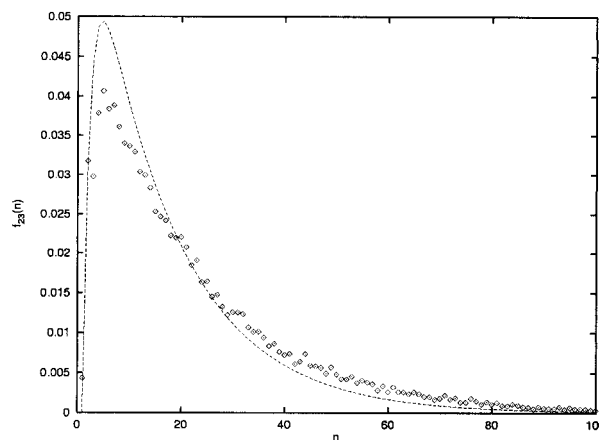
FIG. 16. Probability distributions of the MMT compared with the Markovian predictions [Eq. (A7)] for the model and the parameters of Fig. 15.

mixing times display the same qualitative behavior as the pure diffusive case (cf. Figs. 11 and 13), from which we can deduce that for these features the most relevant effect is due to the diffusive term.

As to the correlation function (Fig. 17), there is a remarkable improvement in catching the correlation functions and the meridional mixing time distribution by means of the Markovian approximation with respect to either the purely chaotic or the purely diffusive case. In general, the presence of diffusion tends to decrease the memory effects so that the Lagrangian dynamics becomes closer to a Markov chain than a purely deterministic case in which nontrivial long-term correlations may render a first-order Markovian approximation inappropriate.

5. Discussion and conclusions

In this paper particle exchange in a meandering jet has been investigated by means of a kinematic model in which mixing is obtained by two different mechanisms: chaotic advection and turbulent diffusion. The large-scale structure of the jetlike flow is assigned in terms of a stationary streamfunction. This has been modified in two ways in order to provide the requested fluid exchange: chaotic advection is induced by adding a time-dependent, relatively small perturbation to the steady portion of the streamfunction. Alternatively, turbulent diffusion has been introduced by superimposing a stochastic field to the latter. The turbulent field has been selected so as to resemble as closely as possible the typical effect of upper ocean turbulence in the absence of coherent structures. Numerical simulations have been carried out for a case in which the two above effects have been jointly present, trying to take into account the richness and complexity of situations ob-

served in the ocean, where the two different mixing mechanisms are thought to be present simultaneously, even if possibly acting at different time and space scales.

The intrinsically different nature of the two investigated mixing mechanisms has resulted in the past in disjointed descriptions of their respective effects: chaotic advection in correspondence of meandering jets has been studied, for example, by means of methods derived from the dynamical systems theory (Pierrehumbert 1991; S92; Wiggins 1992; Duan and Wiggins 1996), whereas the action of turbulent diffusion was addressed by phenomenological Lagrangian motion analysis (B91; DGO93).

In this paper mixing is studied in terms of particle transitions among areas of the physical two-dimensional space characterized by qualitatively different flow regimes, observed as realizations of a Markovian process. Given the structure of the velocity field, the partition of the space accessible to particles is self-evident and physically consistent. A delicate point is obviously the choice
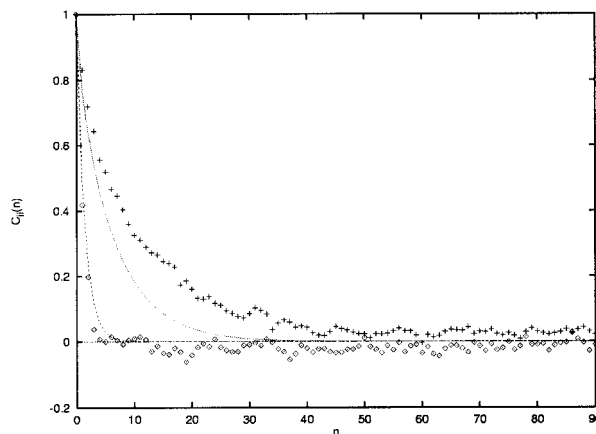
FIG. 17. Correlation functions compared with the Markovian predictions [Eq. (A11)] model and the parameters of Fig. 15.

of the appropriate timescale for sampling the process. However, in our cases an inherent timescale is present in the velocity field, and this is set by, in turn, either the space–time structure of the deterministic portion of the flow (chaotic case) or by the intrinsic memory timescale present in the stochastic velocity field. The Markovian approach is, in this sense, a quite natural one to undertake when looking at the overall mixing from a unified perspective, embedding elements of dynamical systems, and of stochastic process theory. Also, it is an alternative way to look at diffusion avoiding the usual diffusion coefficients, whose general relevance in geophysics has been recently subject to debate (see Artale et al. 1997).

For some fluid exchange properties, the effects of the two above mixing mechanisms are comparable with the results of the Markovian approximation: this is the case, for instance, of the exit times of particles from the jet and the recirculating regions north and south of it. On the other hand, chaotic advection and turbulent diffusion act quite differently, under that perspective, when it comes to meridional mixing and correlation functions. The failure of the Markovian approximation for the characterization of the meridional particle exchange in the chaotic case is due to nontrivial long-term memory effects. Since turbulent diffusion is modeled by a non-white noise process in the stochastic velocity field, we would expect for the turbulent case a closer behavior to that predicted by the Markovian approximation. For the same reason, given the results for the purely chaotic simulations, the combined effect of chaos and diffusion was expected to be well described in Markovian terms. This is indeed the case, and the results for the joint fluid exchange situations agree quite closely with the Markovian predictions.

This qualitative difference between chaotic and diffusive frontal mixing in our process model may contribute to the understanding of previous results: kinematic models typically show relatively strong exchange between jet and recirculating regions and little cross-jet mixing (as mentioned in the introduction: see, e.g., S92 and DGO93). The weakening of long-term memory effects induced by the joint presence of chaotic and turbulent mixing, which is seen in our simulations, makes our results closer to reality with respect to the cases in which only one of the mechanisms is present. In other words, it makes the comparison with transport properties derived from a first-order Markov process even more satisfactory. With increased availability of Lagrangian data in the Gulf Stream, a natural further step will be to apply the technique proposed in this paper to experimental drifter data; this will constitute the subject of future investigation.

It is worth stressing that the possibility of looking in terms of a Markovian approximation at mixing in regions characterized by a quite complex flow structure, even in the presence of different transport mechanisms, can have quite interesting applicative consequences.

When the small-scale details of mixing are beyond our interest, and if and when our flow system shows fairly well-defined timescales, it is apparently possible to look at particle exchange in a relatively simple manner, over timescales that allow for a reduction of the sampling rate. This aspect often turns out to be a critical constraint for the undertaking, for example, of Lagrangian investigations of the real ocean, where reducing the required sampling rate can result in reducing the amount of data to be collected and transmitted.

APPENDIX

Some Properties of Markov Chains

An excellent introduction to Markov chains can be found in Feller (1968). In this appendix we only sum up some formulas that are useful in describing some relevant properties of our system.

A Markov chain is a stochastic process such that the random variables describing state of the system (in our case the cell occupied by the tracer particle) and time are discrete and the probability to be in a given state at time n depends only on the state at time $n - 1$.

All the properties of a Markov chain can be derived from the transition matrix, $\{W_{ij}\}$, whose elements are the probabilities to be in state j at some time n being at time $n - 1$ in state i. For example, the probability to go to state j starting from i in n steps is simply

$$\text{Prob}(i \to j; n) = (W^n)_{ij}. \qquad \text{(A1)}$$

First of all we have

$$\sum_j W_{ij} = 1. \qquad \text{(A2)}$$

In addition to matrix $\{W_{ij}\}$ one can compute the stationary probabilities P_i to visit the cells A_i as elements of the (left) eigenvector corresponding to the eigenvalue 1:

$$P_j = \sum_i P_i W_{ij}. \qquad \text{(A3)}$$

Notice that Eqs. (A2) and (A3) are rather general results that hold for a generic discrete stochastic process. Equation (A2) describes the conservation of probability and Eq. (A3) is nothing but the Bayes theorem. In order to have ergodicity and mixing properties, the Markov

chain must have a nonzero probability to pass through any state in a finite number of steps; that is, there exists a value of n such that $(W^n)_{ij} > 0$ (Feller 1968). Defining $\rho_i(t)$ as the probabilities to visit state i at time t, for a Markov chain, we have

$$\rho_j(t + 1) = \sum_i \rho_i(t)W_{ij}. \tag{A4}$$

In this way one obtains the evolution of the probability vector ρ_i (see Rickman and Froeschlè 1979). Equation (A3) corresponds to $t \to \infty$ in Eq. (A4); that is, the equilibrium distribution $\rho_i(\infty) = P_i$.

The probability of the first exit times from state i can be simply defined as the probability to stay for $n - 1$ steps in state i times the probability to exit at step n; that is,

$$P_i(n) = (1 - W_{ii})(W_{ii})^{n-1}, \tag{A5}$$

which can be rewritten as

$$P_i(n) = \left[\frac{(1 - W_{ii})}{W_{ii}}\right] \exp(-n\alpha), \quad \text{with } \alpha = |\ln W_{ii}|. \tag{A6}$$

In a similar way we can define the probability $f_{ij}(n)$ of the first arrival from state i to state j at step n. This is nothing but the probability to arrive at state j starting from i in n steps, that is, $(W^n)_{ij}$, minus the probability of first arrival at step $n - k$ times the probability of return in k steps, that is, $(W^k)_{jj}$, with $k = 1, \ldots, n - 1$:

$$f_{ij}(n) = (W^n)_{ij} - \sum_{k=1}^{n-1} f_{ij}(n - k)(W^k)_{jj}. \tag{A7}$$

For each state of a Markov process a correlation function can be defined for the variable $\chi_i(n)$, which is equal to 1 if at time n state i is visited and to zero otherwise [see Eqs. (23)–(24)]. The normalized correlation function

$$C_i(n) = \frac{\langle \chi_i(0)\chi_i(n)\rangle - \langle \chi_i(0)\rangle^2}{\langle \chi_i(0)^2\rangle - \langle \chi_i(0)\rangle^2} \tag{A8}$$

is strictly related to the diagonal element $(W^n)_{ii}$ and to the stationary frequency P_i. Notice that

$$\langle \chi_i(0)\rangle = P_i, \qquad \langle \chi_i(0)^2\rangle = P_i. \tag{A9}$$

Furthermore, being P_i the probability that the initial state at $n = 0$ be i and $(W^n)_{ii}$ the probability to be in i again after n iterations, one has

$$\langle \chi_i(0)\chi_i(n)\rangle = P_i \cdot (W^n)_{ii} \tag{A10}$$

and therefore

$$C_i(n) = [(W^n)_{ii} - P_i]/(1 - P_i). \tag{A11}$$

REFERENCES

Artale, V., G. Boffetta, A. Celani, M. Cencini, and A. Vulpiani, 1997: Dispersion of passive tracers in closed basins: Beyond the diffusion coefficient. *Phys. Fluids.,* **9,** 3162–3171.

Backus, R. H., 1986: Biogeographic boundaries in the open ocean. Pelagic Biogeography, UNESCO Tech. Paper Mar. Sci. 49, 9–13. [Available from UNESCO-CSI, 1 rue Miollis, 75732 Paris, France.]

Badii, R., and A. Politi, 1997: *Complexity: Hierarchical Structures and Scaling in Physics.* Cambridge University Press, 318 pp.

Bauer, S., M. S. Swenson, A. Griffa, A. J. Mariano, and K. Owens, 1998: Eddy-mean flow decomposition and eddy-diffusivity estimates in the tropical Pacific Ocean. Part 1: Methodology. *J. Geophys. Res.,* **103,** 30 855–30 871.

Beck, C., and F. Schlögl, 1993: *Thermodynamics of Chaotic Systems.* Cambridge University Press, 306 pp.

Benettin, G., 1984: Power-law behavior of Lyapunov exponents in some conservative dynamical systems. *Physica D,* **13,** 211–220.

——, L. Galgani, A. Giorgilli, and J. M. Strelcyn, 1980: Lyapunov characteristic exponents for smooth dynamical systems and for Hamiltonian systems: A method for computing all of them. *Meccanica,* **15,** 9–24.

Bower, A. S., 1991: A simple kinematic mechanism for mixing fluid parcels across a meandering jet. *J. Phys. Oceanogr.,* **21,** 173–180.

——, and H. T. Rossby, 1989: Evidence of cross-frontal exchange processes in the Gulf Stream based on isopycnal RAFOS float data. *J. Phys. Oceanogr.,* **19,** 1177–1190.

——, and M. S. Lozier, 1994: A closer look at particle exchange in the Gulf Stream. *J. Phys. Oceanogr.,* **24,** 1399–1418.

——, H. T. Rossby, and J. T. Lillibridge, 1985: The Gulf Stream—Barrier or blender? *J. Phys. Oceanogr.,* **15,** 24–32.

Brown, M. G., and R. M. Samelson, 1994: Particle motion in vorticity-conserving, two-dimensional incompressible flows. *Phys. Fluids,* **6,** 2875–2876.

Buffoni, G., P. Falco, A. Griffa, and E. Zambianchi, 1997: Dispersion processes and residence times in a semi-enclosed basin with recirculating gyres. An application to the Tyrrhenian Sea. *J. Geophys. Res.,* **102** (C8), 18 699–18 713.

Cecconi, F., and A. Vulpiani, 1995: Approximation of chaotic systems in terms of markovian processes. *Phys. Lett. A,* **201,** 326–332.

Chandrasekhar, S., 1943: Stochastic problems in physics and astronomy. *Rev. Mod. Phys.,* **15,** 1–89.

Chirikov, B. V., 1979: A universal instability of many-dimensional oscillator systems. *Phys. Rep.,* **52,** 263–379.

Colin de Verdière, A., 1983: Lagrangian eddy statistics from surface drifters in the Eastern North Atlantic. *J. Mar. Res.,* **41,** 375–398.

Cornillon, P., D. Evans, and D. Large, 1986: Warm outbreaks of the Gulf Stream into the Sargasso Sea. *J. Geophys. Res.,* **91,** 6583–6596.

Crisanti, A., M. Falcioni, G. Paladin, and A. Vulpiani, 1991: Lagrangian chaos: Transport, mixing and diffusion in fluids. *La Rivista del Nuovo Cimento,* **14,** 1–80.

Davis, R. E., 1991: Observing the general circulation with floats. *Deep-Sea Res.,* **38,** S531–S571.

del Castillo-Negrete, D., 1998: Asymmetric transport and non-Gaussian statistics of passive scalars in vortices in shear. *Phys. Fluids,* **10,** 576–594.

Dimas, A. A., and G. S. Triantafylou, 1995: Baroclinic-barotropic instabilities of the Gulf Stream extension. *J. Phys. Oceanogr.,* **25,** 825–834.

Duan, J., and S. Wiggins, 1996: Fluid exchange across a meandering jet with quasiperiodic variability. *J. Phys. Oceanogr.,* **26,** 1176–1188.

Dutkiewicz, S., A. Griffa, and D. B. Olson, 1993: Particle diffusion in a meandering jet. *J. Geophys. Res.,* **98,** 16 487–16 500.

Eckmann, J. P., and D. Ruelle, 1985: Ergodic theory of chaos and strange attractors. *Rev. Mod. Phys.,* **57,** 617–655.

Feller, W., 1968: *An Introduction to Probability Theory and its Applications.* Vol. I. Wiley, 528 pp.

Fraedrich, K., 1988: El Niño–Southern Oscillation predictability. *Mon. Wea. Rev.,* **116,** 1001–1012.

——, and K. Müller, 1983: On single station forecasting: Sunshine and rainfall Markov chains. *Beitr. Phys. Atmos.,* **56,** 108–134.

Griffa, A., 1996: Applications of stochastic particle models to oceanographic problems. *Stochastic Modelling in Physical Oceanography,* R. J. Adler, P. Muller, and B. L. Rozovskii, Eds., Birkhäuser, 113–140.

——, K. Owens, L. Piterbarg, and B. Rozowskii, 1995: Estimates of turbulence parameters from Lagrangian data using a stochastic particle model. *J. Mar. Res.,* **53,** 371–401.

Halliwell, G. R., and C. N. K. Mooers, 1983: Meanders of the Gulf Stream downstream from Cape Hatteras. 1975–1978. *J. Phys. Oceanogr.,* **13,** 1275–1292.

Khinchin, A. I., 1957: *Mathematical Foundations of Information Theory.* Dover, 120 pp.

Kluiving, R., H. W. Capel, and R. A. Pasmanter, 1992: Symbolic dynamics of fully developed chaos I. *Physica A,* **183,** 67–95.

Kontoyiannis, H., and D. R. Watts, 1994: Observations on the variability of the Gulf Stream path between 74°W and 70°W. *J. Phys. Oceanogr.,* **24,** 1999–2013.

Lacorata, G., R. Purini, A. Vulpiani, and E. Zambianchi, 1996: Dispersion of passive tracers in model flows: Effects of the parametrization of small-scale processes. *Ann. Geophys.,* **14,** 476–484.

Lee, T., 1994: Variability of the Gulf Stream path observed from satellite infrared images. Ph.D. dissertation, University of Rhode Island, 188 pp.

Levinson, H. F., 1991: The long-term dynamical behavior of small bodies in the Kuipter belt. *Astron. J.,* **102,** 787–794.

Lichtenberg, A. J., and M. A. Lieberman, 1992: *Regular and Chaotic Dynamics.* Springer, 692 pp.

MacKay, R. S., J. D. Meiss, and I. C. Percival, 1987: Resonances in area-preserving maps. *Physica D,* **27,** 1–20.

Mannella, R., and V. Palleschi, 1989: Fast and precise algorithm for computer simulation of stochastic differential equations. *Phys. Rev.,* **A40,** 3381–3386.

Meiss, J. D., and E. Ott, 1986: Markov tree model of transport in area-preserving maps. *Physica D,* **20,** 387–402.

Nicolis, C., W. Ebeling, and C. Baraldi, 1997: Markov processes, dynamic entropies and statistical prediction of mesoscale weather regimes. *Tellus,* **49A,** 108–118.

Okubo, A., 1971: Oceanic diffusion diagrams. *Deep-Sea Res.,* **18,** 789–802.

Olson, D. B., 1991: Rings in the ocean. *Ann. Rev. Earth Planet. Sci.,* **19,** 283–311.

Pierrehumbert, R. T., 1991: Chaotic mixing of tracers and vorticity by modulated travelling Rossby waves. *Geophys. Astrophys. Fluid Dyn.,* **58,** 285–319.

Pope, S. B., 1994: Lagrangian PDF methods for turbulent flows. *Ann. Rev. Fluid Mech.,* **26,** 24–63.

Poulain, P. -M., and P. P. Niiler, 1989: Statistical analysis of the surface circulation in the California Current System using satellite-tracked drifters. *J. Phys. Oceanogr.,* **19,** 1588–1603.

Rickman, H., and C. Froeschlè, 1979: Orbital evolution of short-period comets treated as a Markov process. *Astron. J.,* **84,** 1910–1917.

Risken, H., 1989: *The Fokker–Planck Equation.* Springer, 472 pp.

Samelson, R. M., 1992: Fluid exchange across a meandering jet. *J. Phys. Oceanogr.,* **22,** 431–440.

Thomson, D. J., 1986: A random walk model of dispersion in turbulent flows and its application to dispersion in a valley. *Quart. J. Roy. Meteor. Soc.,* **112,** 511–530.

——, 1987: Criteria for the selection of stochastic models of particle trajectories in turbulent flows. *J. Fluid Mech.,* **180,** 529–556.

Tracey, K. L., and D. R. Watts, 1986: On Gulf Stream meander characteristics near Cape Hatteras. *J. Geophys. Res.,* **91,** 7587–7602.

van Dop, H., F. T. M. Niewstadt, and J. C. R. Hunt, 1985: Random walk models for particle displacements in inhomogeneous unsteady turbulent flows. *Phys. Fluids,* **28,** 1639–1653.

Vazquez, J., and D. R. Watts, 1985: Observations on the propagation, growth and predictability of Gulf Stream meanders. *J. Geophys. Res.,* **90,** 7143–7151.

Verron, J., and K. D. Nguyen, 1989: Lagrangian diffusivity estimates from a gyre-scale numerical experiment on float tracking. *Oceanol. Acta,* **12,** 167–176.

Watts, D. R., 1983: Gulf Stream variability. *Eddies in Marine Science,* A. Robinson, Ed., Springer Verlag, 114–144.

Wiggins, S., 1992: *Chaotic Transport in Dynamical Systems.* Springer, 352 pp.

Yang, H., 1996: Chaotic transport and mixing by ocean gyre circulation. *Stochastic Modelling in Physical Oceanography,* R. J. Adler, P. Muller, and B. L. Rozovskii, Eds., Birkhäuser, 439–466.

Yeung, P. K., and S. B. Pope, 1989: Lagrangian statistics from direct numerical simulations of isotropic turbulence. *J. Fluid Mech.,* **207,** 531–586.

Zambianchi, E., and A. Griffa, 1994a: Effects of finite scales of turbulence on dispersion estimates. *J. Mar. Res.,* **52,** 129–148.

——, and ——, 1994b: On the applicability of a stochastic model for particle motion to drifter data in the Brazil–Malvinas extension. *Annali Ist. Univ. Navale,* **61,** 75–90.